XIX. Results of Basic Improvements to the Extraction of Spectra from IUE Low Dispersion Images

R.C. Bohlin, D.J. Lindler, and B.E. Turnrose

ABSTRACT

Since the chances for a long additional lifetime for the IUE Satellite seem good, the data reduction system in use at the NASA and ESA ground stations is being optimized in order to realize the full capabilities of the observatory. The new software for extraction of low dispersion spectra has been extensively tested and is now ready for implementation in production data processing. The photometry and, therefore, the absolute calibration are unchanged. The single most important improvement is an increase in apparent resolution, achieved by doubling the number of points at which the spectrum is sampled. For example, a pair of emission lines separated by two sample points are unresolved in the old method, but are clearly distinguished when the four samples of the new method are displayed. In addition, an astronomer will find numerous other benefits on future IUE standard data tapes. Some examples are complete sampling of the data, improved backgrounds used to compute net spectra, and correct extraction of spectra of diffuse sources where the spectral lines are tilted with respect to the dispersion direction. The flagging of anomalous segments of extracted spectra is upgraded, and more useful information is now included in the header records using a format that is easily read by most computer systems. All changes to the IUE standard data tape format should be transparent to the user, except for the increase in the physical record length, necessitated by the increase in the number of spectral sample points.

1. Summary of the Old and New Techniques

The first step in reducing IUE data is to convert from the raw, non-linear image in Data Number (DN) units to linearized Flux Number (FN) units. The following subsections describe the differences between the old and new photometric correction techniques, which apply to both low and high dispersion images. The second step is to extract a spectrum from the photometrically corrected image. Only the case of low dispersion extraction is described for the old and new methods. See Lindler and Bohlin (1980) for more details.

1.1 Old Method

The first processing step for each image is a geometric correction of the raw image performed by means of bilinear interpolation within a square grid of 169 fiducial masks (reseaux). This correction involves a resampling of the original image, resulting in some degradation of resolution. Since this resampling is done in the (non-linear) DN space of the raw image, some photometric error is also introduced. The photometric correction of the image is effected by means of a pixel-by-pixel intensity transfer function. The spectral data are then extracted with a slit width of 1.4 pixels, once per image line with a slit centered on the pixel that lies closest to the intersection of that scan line and the dispersion line. Since the low dispersion spectra lie at $38^{\circ} \pm 1$ to the scan lines, about 13% of the spectral information is not extracted. The background is smoothed with a triangular filter before subtraction to obtain the net spectrum.

1.2 New Method

In the new method the resampling of the raw image is avoided by performing the photometric correction without prior geometric correction. Using the square grid of 169 reseaux the correct ITF can be associated with each pixel. The raw data pixel will have a position between four ITF curves. Each of these ITF's is applied to the pixel DN value and bilinear interpolation of the four values yields the flux value. To extract the spectrum from the photometrically corrected image it is

necessary to use dispersion constants for a geometrically corrected image. This is done by computing the position of a given wavelength in "geomed" space and then using the information from the reseaux grid to compute the position in "raw" space. The flux value assigned is the bilinear interpolation of the flux values of the four pixels around the computed raw position. A spacing of 0.7 pixels both parallel and perpendicular to the dispersion is used relative to the geometrically correct coordinates. Neighboring points are added in the spatial direction, giving a spacing perpendicular to the dispersion of 1.4 pixels as in the old method, but retaining the higher sampling frequency of 0.7 pixels in wavelength. The image is completely sampled without losing any information. Furthermore, the spectra are sampled with a uniform spacing between points, in contrast to the variable spacing produced by the old technique. The gross and the background spectra are then obtained by summing the appropriate regions in the spatial direction. The background is then smoothed using a median filter followed by a triangular filter.

2. Improvements in Resolution

2.1 Narrow Features

The single most pronounced enhancement in scientific return of the new method is the increase in apparent resolution. Figure 1 shows a region of a platinum wavelength calibration spectrum extracted with the old and new method. The pair of emission lines, which can be seen as two distinct features on an image near 2040Å is unresolved with the old method but is clearly separated with the new method. The increased resolution is due to not resampling the image for geometrical correction and to using an extraction slit and corresponding sample spacing of one half of the old slit width and spacing.

Because of the narrower extraction slits in the new method, the noise in extracted spectra is increased by a factor of about 1.4, as expected. However, the guest investigator will have the option of binning the data to reduce noise or co-adding multiple exposures to obtain a significantly improved resolution.

2.2 Broad Features

The old IUE software suffers from deficiencies in the computation of the background spectrum in the case where the background is a significant fraction of the gross extracted spectrum. The problem is manifested by a broad dip or rise in the net spectrum, because the background, which includes reseaux and noise spikes, is smoothed by a broad triangular filter. In the new software, neither reseaux nor saturated pixels are used in computing the background. Instead, the background for contaminated points will be filled by interpolation between neighboring values. In addition, residual noise spikes will be removed by a median filter (Schiffer and Holm, 1980). The width of the median filter is 63 points followed by a mean filter done twice (triangular filter) with a width of 31 points (Turnrose, Harvel, and Bohlin, 1979).

Another deficiency of the old software occurs in the computation of the background near the target ring of the image. At the edge of the TV target, the symmetric background used in the past included regions outside the data circle. If only one side of the spectrum lies within the valid circle of data, the new background is taken asymmetrically. Furthermore, a smoothing of this background to suppress noise is accomplished by extending the first or last fully smoothed point to either end of the array. The amount of the extension is 31 and 15 points for the median and mean filters, respectively. The main scientific benefit of the improved background at the endpoints is to extend the good region of the SWP net spectrum to 1990Å from about 1955Å where a broad dip often began with the old software.

2.3 Diffuse Source Spectra

In both the long and short wavelength spectrographs, the orientation of the entrance apertures is such that neither the major axis of the large aperture nor the axis defined by the lines joining the centers of the large and small apertures are normal to the direction of the dispersion in the low resolution mode. The true orientations are illustrated in Figure 2, in which the "omega angles" ω_L and ω_S are defined. Theta is the angle which defines the orientation of the spectra on the camera faceplate in geomed coordinates.

Table 1 lists the numerical values of these angles. The values in Table 1 were derived from geometrically corrected Pt-Ne lamp exposures, where both apertures should be uniformly illuminated. Note that the apparent ω angles as measured on a raw image differ by up to 4° from those in Table 1.

Table 1. Omega Angles in Degrees

Camera	ω_L	ω_S	θ
LWR	97	83	53
SWP	81	92.5	129

When low dispersion spectra are extracted from the geometrically and photometrically corrected images, the assignment of wavelengths to successive spatial segments ("pseudo-orders") of the spatially-resolved spectra is done with respect to lines of constant wavelength whose orientation is defined by means of the parameter ω. Since all omega angles have been set at 90° in the past, the optimum resolution of diffuse source spectra in the large aperture has not been realized; and the wavelengths assigned to pseudo-orders of diffuse sources is correct only for the central order. For small-aperture observations, the values ω_S are used, thereby assigning the same wavelength (to within $\sim 1\text{Å}$) to the center of the large aperture and the center of the small aperture. In the new software the above omega angles are used for all point and diffuse source spectra. The trailed spectra remain at $\omega_L = 90^{\circ}$, and separate schemes will be used for production processing of trailed spectra.

3. Changes in Photometry

3.1 Relative Photometry

Since the new extraction slit is only one-half as wide as the old slit the net signal extracted in FN units should be nominally one-half that obtained in an old extraction. However, the new FN values are multiplied by 2 to normalize them to the old slit width and for ease in comparing the results of the two methods. A set of evaluation

spectra were processed with both the old and new software using identical reseaux data sets and dispersion constants. The results of the comparisons are summarized in Figures 3 and 4, which show the ratio of OLD/NEW photometry in 100Å bands for the SWP and LWR camera, respectively. The evaluation spectra are of hot standard stars, as detailed in Table 2. The most important sets of ratios are for the top 3 spectra of large aperture (L-Ap) point sources, because this mode of observation at the nominal 100% exposure defines the overall level of the absolute calibration. A reseau in the faint 1200Å band of SWP and a bright spot in the 2200Å band of LWR complicate those large aperture comparisons. The smaller open circles on the second 100% comparison are a check for 25Å bands to verify that the broader 100Å bands are not masking any serious change on a more localized scale.

In summary, Figure 3 and 4 do not show any systematic change greater than 2% in level or shape at the 100% exposure level. At the 120% level extrapolation in the ITF (see Section 4.1) effects the points near the sensitivity peaks around 1300Å in SWP and 2700Å in LWR. The changes shown for high background spectra are somewhat larger, and are caused mostly by the improved background treatment.

3.2 Linearity

Because of the significant changes in net FN for high background spectra and because of the possibly significant effects of extrapolation, Figure 5 was constructed; however, it demonstrates that the linearity of IUE data has not changed appreciably at 1300Å in SWP where extrapolation would have maximum effect and at 2100Å in LWR where low IUE sensitivity makes linearity particularly important. The results show that, for the weakest SWP exposures around the 10% relative exposure level, the derived FN are too low by 15 to 20% in comparison to what they would be for perfect linearity (unity in Figure 5). The weakest LWR exposures are too high by a similar amount and show the same non-linearity as in the original evaluation in Figure 9 of Bohlin, et al. 1980. On the other hand, the difference for SWP between Figure 9 of Bohlin, et al. and Figure 5 here represents the change in linearity due to the SWP ITF correction (Holm 1979). Figure 5 shows little difference between the linearity of old and new processing or between point source and trailed spectra.

This residual non-linearity of IUE data is probably the most serious deficiency of the system. The agreement between the new and old non-linearities demonstrates that the source of this error is not in the processing software. The problem must lie in the construction of the ITF that is supposed to linearize the data or in the fundamental assumption that an ITF constructed from flat fields can be used to linearize spectral images.

3.3 Absolute Calibration

Because Figures 3 and 4 illustrate that the new software changes the signal extracted from IUE images by less than 2% at a level near 100% exposure, the overall sensitivity of the system is unchanged and no new derivation of the absolute calibration is needed. However, the occasion of the implementation of the new low dispersion processing has been chosen to change the absolute calibration, as applied to the output tapes and plots, from the original to the revised absolute calibration as defined by Bohlin and Holm (1980) in May 1980.

4. Special Data Flags

4.1 Extrapolation

The problem with extrapolation of the ITF beyond the last two valid points has been discussed by Turnrose, Harvel, and Bohlin (1980). Two improvements in this regard are implemented in the new reduction system. First, the dynamic range of the possible extrapolation has been greatly extended. Second, the output products are flagged where extrapolation occurs. Both of these improvements are possible because of special coding used in the photometrically corrected image (Turnrose, Bohlin, and Lindler 1980).

4.2 Saturation

Because no resampling of the raw image occurs in a geometric correction, all of the saturated pixles at 255 DN remain and can be flagged in the photometrically corrected image and the output products. In addition, the flag for a saturated pixel is no longer a FN value of

32767; rather, the FN value is calculated in a continuous fashion such that a saturated emission line would tend to have a flat top in analogy with a saturated image on film.

4.3 Reseaux

The flagging of reseaux in extracted spectra has been improved in two ways. First, reseaux are not flagged in background spectra, since they are not used in that computation, as discussed in Section 2.2. Second, the amount of data affected by reseaux is again reduced due to the decreased effective size of each reseau. The reseau size remains small because of the lack of any resampling in a geometric correction and because of the removal of the artifact of the old software that caused reseaux to expand in going from the gross to the net spectrum.

5. Expanded Header Information

Additional information pertinent to the astronomical interpretation of the data has been placed in the header records, leaving the position and definition of previously used quantities essentially unchanged.

5.1 VICAR Header

The content of the 360 byte records at the beginning of the data files on an IUE magnetic tape (VICAR header) is modified to reflect the names of the new reduction programs. The midpoint of the date of the observation, the target coordinates, and a statement of either a manual or automatic shift of the dispersion constants have been added and will also appear on the alphanumeric information written on standard Calcomp plots. The format of the numerical data such as the slit height and dispersion constants in the VICAR header is unchanged in order to maintain transparency with any existing software that may decode this header.

5.2 Data Header Record

Immediately following the VICAR header on the magnetic tape files of extracted spectra is the 2048 byte (1204 bytes in the old software) data header record, otherwise known as record zero because of the

order of the spectral information which begins with record number one. Since this record consists entirely of 16 bit integer numbers and is particularly easy to read on most computers, the content of this record has been greatly expanded to include most numerical quantities needed for automatic data processing. Certain quantities are unavailable for old images, including the observation date, target coordinates, and temperature of the head amplifier (THDA). Table 3 gives the first image number for each of the 4 cameras for which the above 3 quantities are generally correct for NASA images. Any reprocessing of old data with the new software will result in zero for these 3 quantities. Other examples of newly available information in record zero are date of image processing, omega angle, slit height and placement information, dispersion constants, and an auto or manual shift indicator. See Turnrose, Bohlin, and Lindler (1980) for format details.

Acknowledgements: Mr. R.W. Thompson and Mr. B.T. Coulter did an excellent job of organizing the processing and reduction of large amounts of evaluation data through many iterations during the development testing of the new software.

Table 2

Spectra Used in Figures 3 and 4

Star	Image	Aper.	Exp. Time (sec)	Comment
BD+33°2642	SWP2061	L	285	120% Point Source
	SWP4003	L	240	100% " "
	"	S	400	∿100% " "
	SWP4007	L	71.7	30% " "
	LWR1859	L	225	120% " "
	LWR3561	L	190	100% " "
	"	S	317	∿100% " "
	LWR3565	L	56.9	30% " "
HD60753	SWP6822	L	9.83	100% Point Source
	SWP3219	L	40.8	100% Trail
	SWP3239	L	3.69	On High Background
	LWR1974	L	9.83	100% Point Source
	LWR2822	L	31.2	100% Trail
	LWR2821	L	2.87	On High Background
HD93521	SWP1955	L	2.87	100% Point Source
	LWR1805	L	2.87	100% " "

L - Large Aperture Spectrum

S - Small Aperture Spectrum

Table 3

First Image Numbers for Correct Presence

of the Specified Quantities

Quantity	Image Numbers for			
Camera:	1(LWP)	2(LWR)	3(SWP)	4(SWR)
Midpoint of Observation	1179	4222	4907	1154
THDA	1179	4015	4625	1154
Target Coordinates	1194	6385	7397	1157

REFERENCES

Bohlin, R.C., and Holm, A.V. 1980, "Photometric Calibration of the IUE VIII. Comprehensive Revision to the IUE Absolute Calibration in Low Dispersion," IUE NASA Newsletter No. 10, 37.

Bohlin, R.C., Holm, A.V., Savage, B.D., Snijders, M.A.J., and Sparks, W.M. 1980, Astron. and Astrophys., 85, 1-13.

Holm, A.V. 1980, "Notification of an Error in the Photometric Correction of SWP Images," IUE NASA Newsletter No. 7, 27.

Lindler, D.J., and Bohlin, R.C. 1981, in The Universe at Ultraviolet Wavelengths: The First Two Years of IUE, ed. R.D. Chapman (NASA CP).

Schiffer, F.H., and Holm, A.V. 1980, "A Median Filter Subroutine," IUE NASA Newsletter No. 8, 41.

Turnrose, B., Bohlin, R., and Lindler, D. 1980, "IUE Data Reduction XVIII. Implementation of New Low Dispersion Software: Summary of Output Format Changes," IUE NASA Newsletter No. 12, in press.

Turnrose, B., Harvel, C., and Bohlin, R. 1979, "IUE Data Reduction X. Planned Changes to the Background Smoothing Algorithm," IUE NASA Newsletter No. 7, 9.

Turnrose, B., Harvel, C., and Bohlin, R. 1980, "IUE Data Reduction XIII. Modification of Photometric Correction to Extrapolate the Intensity Transfer Function," IUE NASA Newsletter No. 8, 32.

FIGURE CAPTIONS

Fig. 1 -- Comparison of a portion of a LWR platinum lamp spectrum extracted with the new and old extraction methods. The symbol "+" marks extraction positions, i.e. data points that are on the guest observer data tapes. Some of the stronger lines that are seen in high dispersion are identified by a vertical line on the new method plot with a length approximately proportional to the observed high dispersion line strength. The positions of these lines are shifted about 3Å longward to account for the thermal shift of one pixel between LWR 6153 and the mean dispersion constants.

Fig. 2 -- Format of the low dispersion TV images with sample number increasing to the right and line number increasing downward. With respect to the low resolution dispersion line, ω_L is the angle of the major axis of the large aperture and ω_S is the angle of the line joining points with the same wavelengths for objects centered in the large and small apertures.

Fig. 3 -- Filled Circles: ratios of IUE response as extracted for the old and new software in 100Å bands for the SWP camera.
Open Circles: The same ratios in 25Å bands.

Fig. 4 -- Same as Fig. 3 for the LWR camera.

Fig. 5 -- The deviation of the points from unity in relative response is the measure of non-linearity at the various exposure levels. The trends for wavelengths other than those illustrated are generally similar.

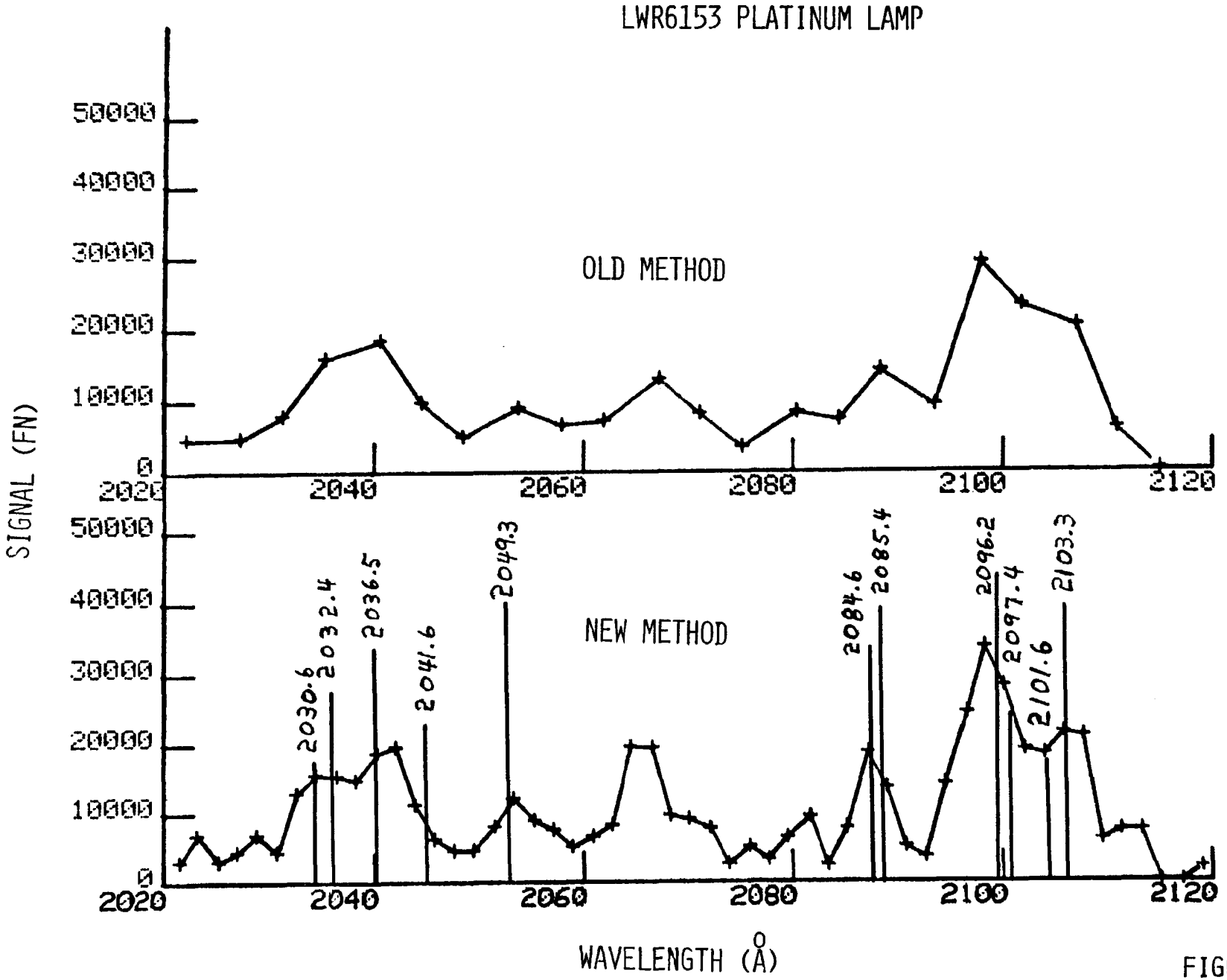
LWR6153 PLATINUM LAMP
OLD METHOD
NEW METHOD
SIGNAL (FN)
WAVELENGTH (Å)
50000
40000
30000
20000
10000
0
2020
2040
2060
2080
2100
2120
2030.6
2032.4
2036.5
2041.6
2049.3
2084.6
2085.4
2096.2
2097.4
2101.6
2103.3

FIGURE 1

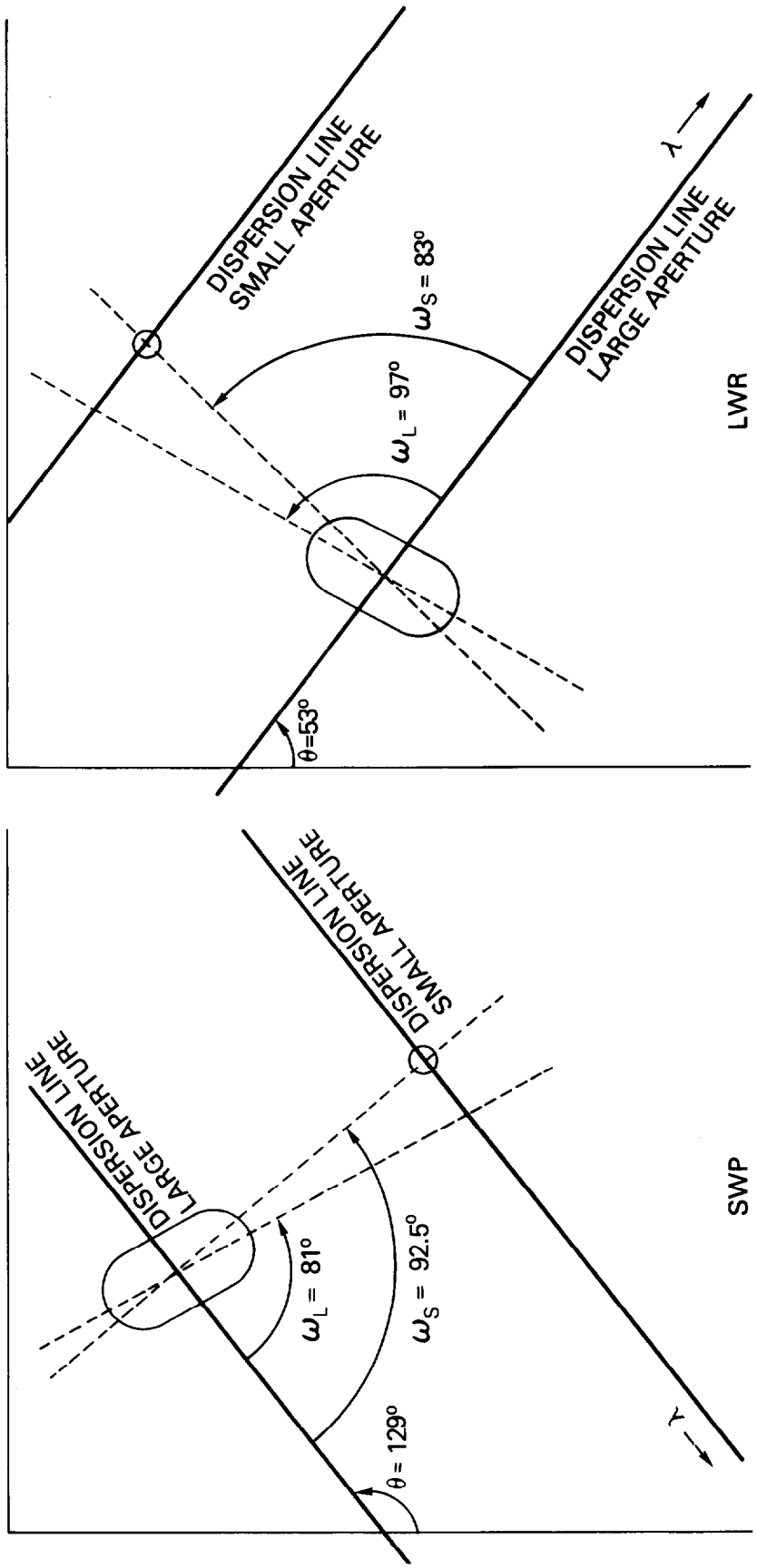
DISPERSION LINE
SMALL APERTURE
DISPERSION LINE
LARGE APERTURE
λ
$\omega_S = 83°$
$\omega_L = 97°$
θ=53°
LWR
DISPERSION LINE
SMALL APERTURE
DISPERSION LINE
LARGE APERTURE
$\omega_L = 81°$
$\omega_S = 92.5°$
θ = 129°
γ
SWP

FIGURE 2

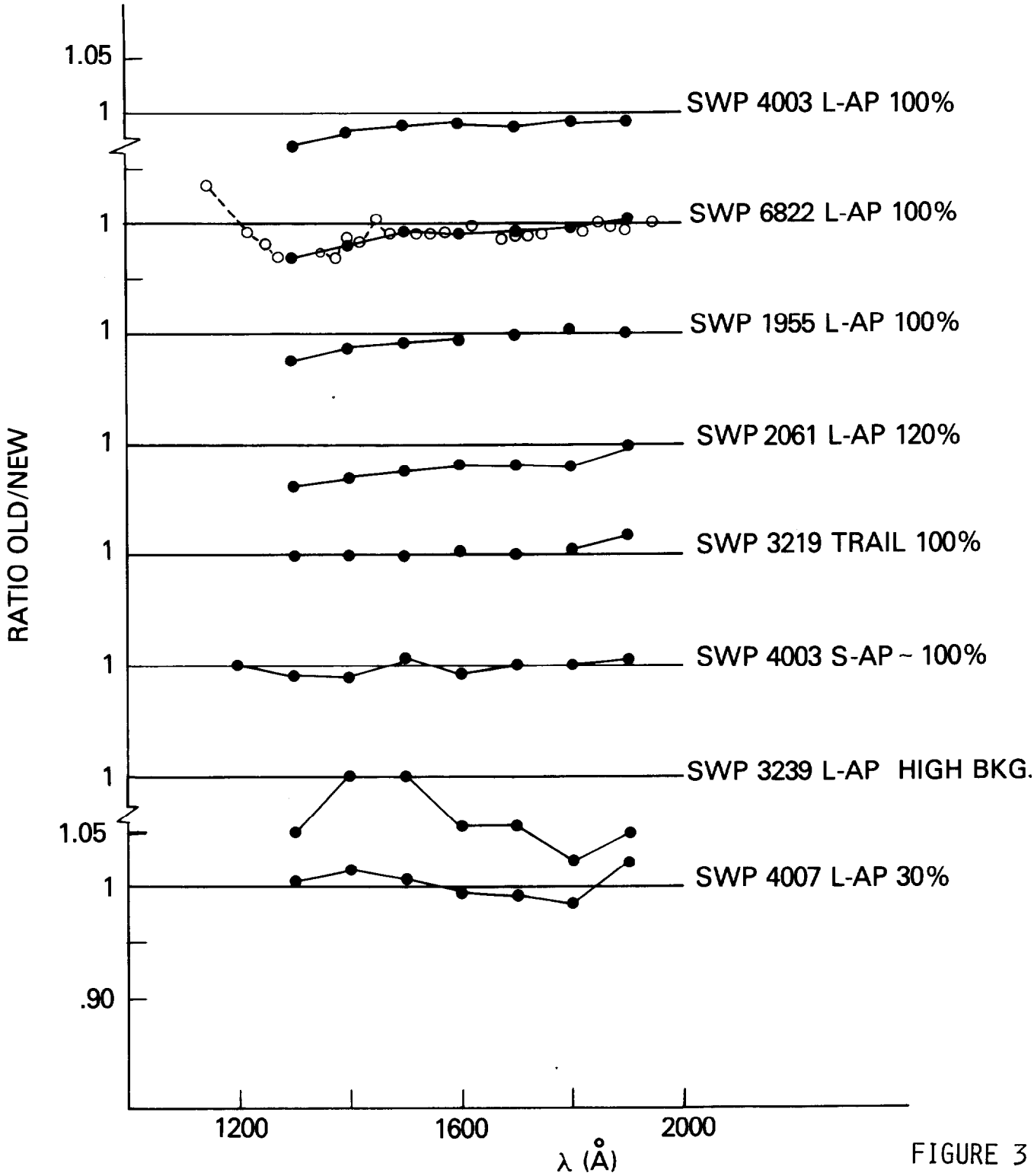
RATIO OLD/NEW
1.05
1
1
1
1
1
1
1
1
1.05
1
.90
SWP 4003 L-AP 100%
SWP 6822 L-AP 100%
SWP 1955 L-AP 100%
SWP 2061 L-AP 120%
SWP 3219 TRAIL 100%
SWP 4003 S-AP ~ 100%
SWP 3239 L-AP HIGH BKG.
SWP 4007 L-AP 30%
1200
1600
2000
λ (Å)

FIGURE 3

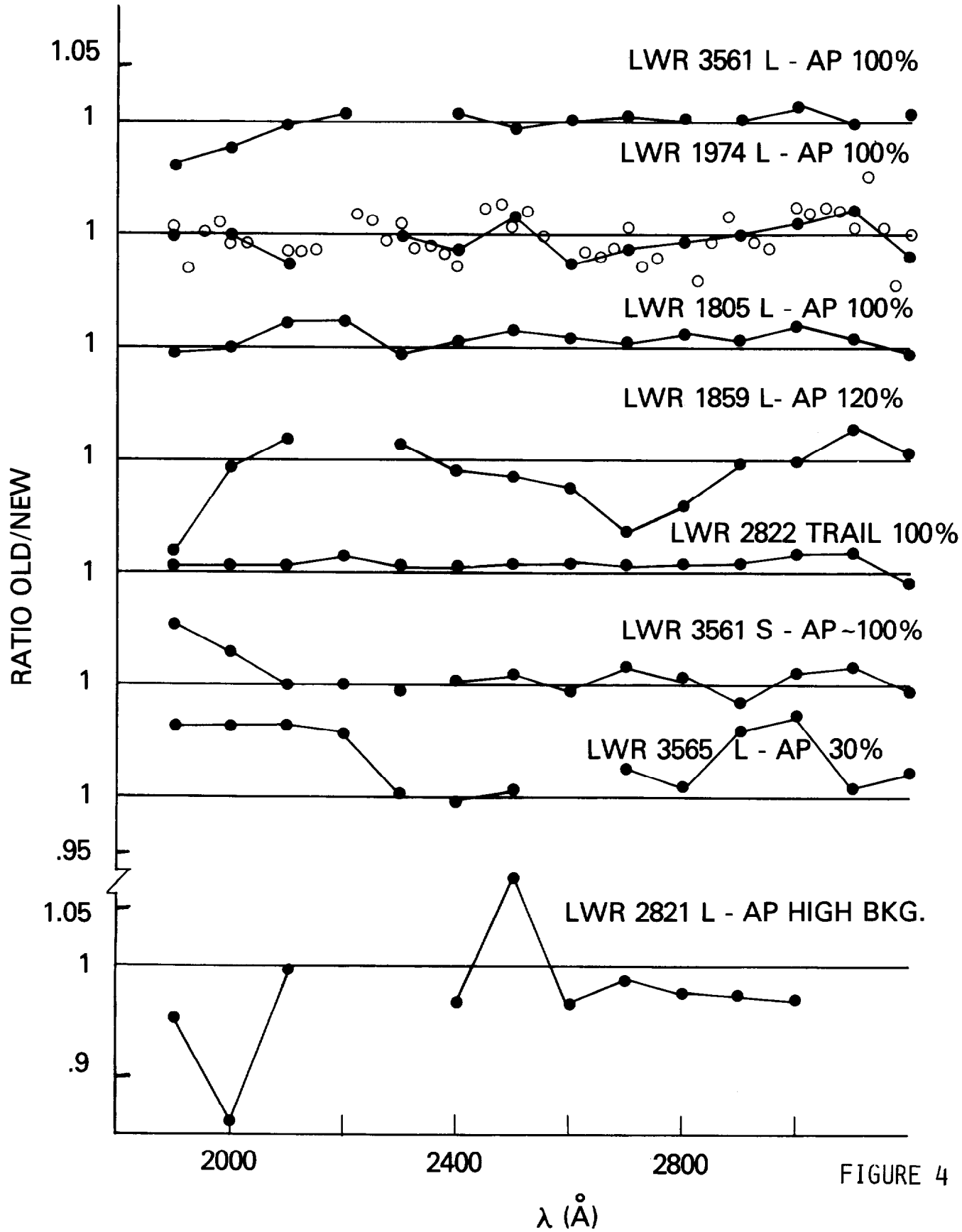
1.05
1
1
1
1
1
1
.95
1.05
1
.9
RATIO OLD/NEW
LWR 3561 L - AP 100%
LWR 1974 L - AP 100%
LWR 1805 L - AP 100%
LWR 1859 L- AP 120%
LWR 2822 TRAIL 100%
LWR 3561 S - AP~100%
LWR 3565 L - AP 30%
LWR 2821 L - AP HIGH BKG.
2000
2400
2800
λ (Å)

FIGURE 4

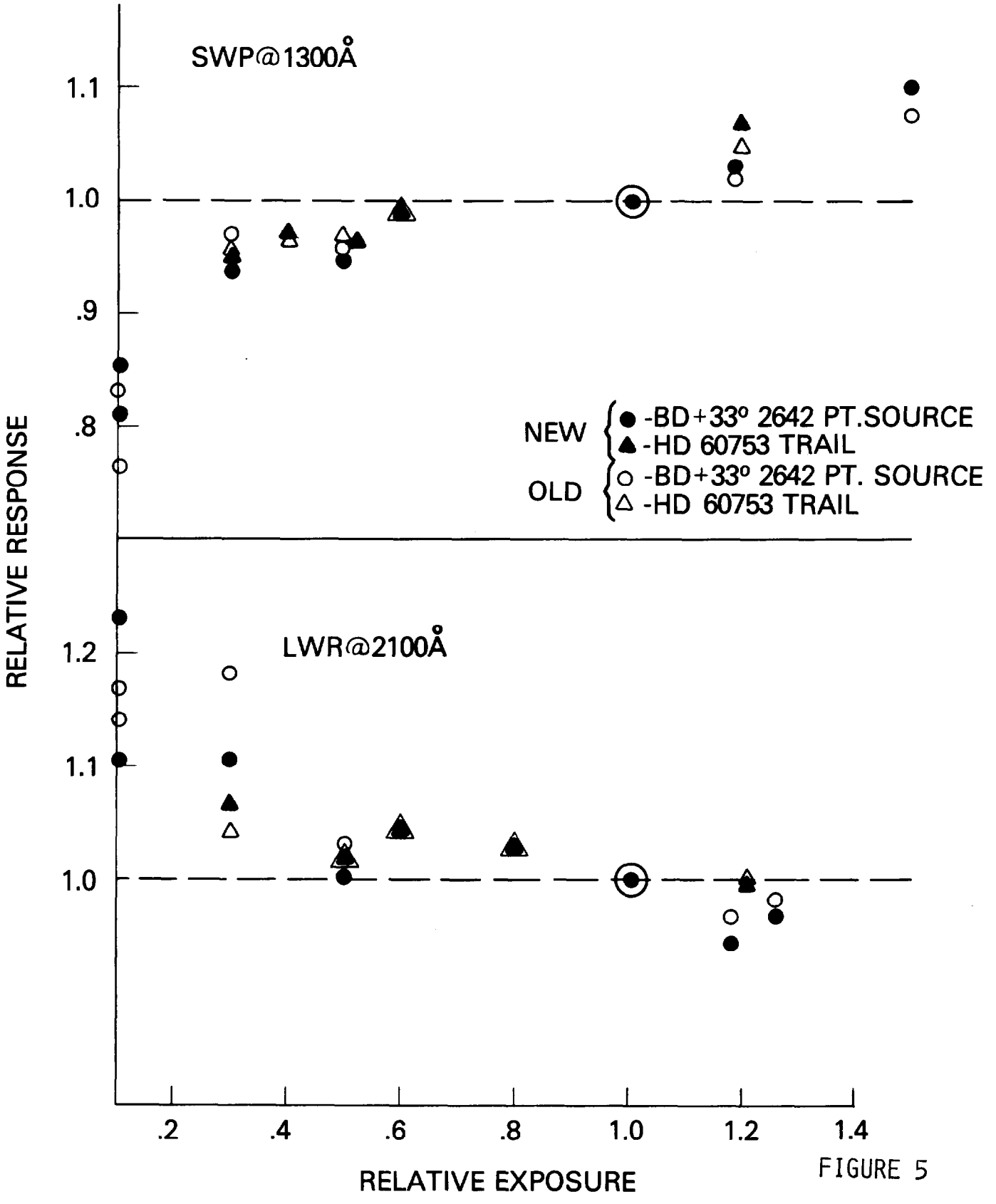
SWP@1300Å
1.1
1.0
.9
.8
NEW
● -BD+33° 2642 PT.SOURCE
▲ -HD 60753 TRAIL
OLD
○ -BD+33° 2642 PT. SOURCE
△ -HD 60753 TRAIL
LWR@2100Å
1.2
1.1
1.0
RELATIVE RESPONSE
.2
.4
.6
.8
1.0
1.2
1.4
RELATIVE EXPOSURE

FIGURE 5